

Spectroscopic Characteristics of the Cationic Dye Basic Orange 21 in Leukocytes

Z. Eizig¹, D. T. Major², H. L. Kasdan³, E. Afrimzon¹, N. Zurgil¹ and M. Deutsch¹

¹The Biophysical Interdisciplinary Jerome Schottenstein Center for the Research and the Technology of the Cellome, Physics Department, Bar Ilan University, Ramat Gan, Israel

²Department of Chemistry, Bar-Ilan University, Ramat-Gan, Israel

³IRIS Diagnostics Division, IRIS International Inc., Chatsworth, CA, U.S.A.

1 STAGE OF THE RESEARCH

A comprehensive literature review regarding BO21 and other metachromatic dyes has been completed and yields many open questions regarding the cause for BO21 metachromasia. Recognizing the need for a more satisfactory basis for machine interpretation of leukocytes, Kass (Kass, 1986) found useful, reaction properties of Basic Orange #21 (BO21), which acts supravivally to induce metachromasia in leukocytes.

However, surprisingly, and most probably due to the low quantum yield of BO21, reference to its fluorescence characteristics and polarization is missing.

Therefore, the spectroscopic aspect of BO21 is extensively investigated in our work. First, the dependency of BO21 metachromasia upon a variety of factors (pH, viscosity, salts, proteins temperature, etc.) have been investigated. In all experiments, phosphate buffered saline buffer (PBS) was used as the hosting medium in order to retain a constant pH level.

At first, the influence of these factors upon BO21 was assessed by changes (red or blue shift) in the absorption spectrum of BO21. Practically, the ratio between the absorption (A) measured within the wavelength windows 481 – 490nm and within 461 – 470nm was calculated for suspending media without (S) and with reagent (R), after which the Absorption Ratio (AR) was calculated (Equation 1).

$$AR = \frac{A(481-490)/A(461-470)_S}{A(481-490)/A(461-470)_R} \quad (1)$$

Though some influence of the acidity level and the viscosity could be observed via the ARs ratio, they were negligible in respect to that obtained with heparin, an anion organic molecule which exists in some types of leukocytes. It has been found that heparin induces a blue shift in the absorption

spectrum (AR ~ 0.84), yielding a red hue BO21 solution. Results are summarized in Table 1.

The absorption (solid line) and emission (dashed line) spectra of BO21 in the absence (blue curves), and in the presence (red curves) of heparin, are shown in Figure 1. The measured absorption wavelength windows are indicated by the blue blocks.

Table 1: Influence of factors upon BO21 absorption spectra.

Variable	Reference	Variable density	Abs. Ratio
Concentration	10uM BO21	50uM	1.00
pH	pH 7.4	pH 5	0.99
pH	pH 7.4	pH 9	1.00
Viscosity	1cP	219cP	1.07
CaCl ₂	BO21 in H ₂ O	0.09 uM	1.00
CuSO ₄	BO21 in H ₂ O	1.35nM	1.00
KCl	BO21 in H ₂ O	600mM	1.00
MgCl ₂	BO21 in H ₂ O	70 mM	1.00
NaCl	BO21 in H ₂ O	300 mM	1.00
BSA/PBS	BO21 in PBS	100 uM	1.04
BSA/H ₂ O	BO21 in H ₂ O	100 uM	1.01
heparin	BO21 in H ₂ O	0.8 uM	0.84

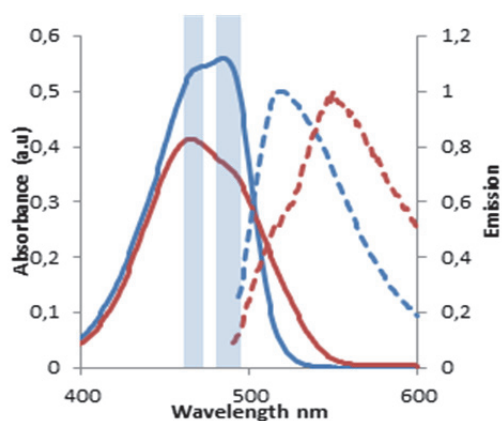


Figure 1: absorption (solid line) and emission (dashed line) spectra of BO21 (10uM) in the absence (blue) and in the presence (red) of 0.8uM heparin. The two orthogonal blocks represent the said wavelength windows.

Next, it was found that in the presence of heparin the emission peak of BO21 was extremely red shifted; from 519 to 550nm for excitation of BO21 at 490nm.

Finally, Fluorescence polarization (FP) measurements of BO21 in water yielded, contrary to all expectations, $FP \sim 0.450$. However, the presence of heparin produced a dramatically lower FP; about 0.200.

1.1 Mechanism

Changes in absorption spectrum might evolve from electrostatic bonds between BO21 molecules (formation of dimers, trimers, etc.), as well as the presence of heparin, on which the dye cation aggregates, occupying adjacent sites on the polyanion. In order to distinguish between the two possible mechanisms, two types of experiments were performed. First, the electrostatic bonds between BO21 and heparin were neutralized by replacing the heparin with small anion molecules. Results are listed in Table 2. As can be seen, no influence of the salts upon BO21 absorbance could be observed; the control (BO21 in water or in PBS) values (~ 0.59) were, for all practical purposes, the same as with salts (3rd column from left). Moreover, the presence of heparin caused no noticeable change as well (4th column from left).

Table 2: Influence of anion and cation salts upon BO21 absorption spectra with and without heparin.

Sub.	Concentration	Absorbance at 484nm	
		BO21+ Sub.	BO21+ Sub.+ heparin
H ₂ O	control	0.59	0.49
PBS	control	0.57	0.57
(NH ₄) ₂ SO ₄	0.2M	0.58	0.59
NaAC	0.2M	0.58	0.59
NaCl	0.2M	0.58	0.58
Sub.- Substance			

Next, the role of BO21 aggregation in metachromasia was examined independently by tracing the dependency of BO21 absorption upon its concentration. In order to avoid measurement errors due to inner filter effects, a special cuvette was designed with an optical path of 0.15mm. In Figure 2, two cuvettes are shown, each containing the same BO21 concentration. Nevertheless, with the regular 1cm cuvette (item a in the figure) a red shift is evident due to enhanced inner filter effect, while with the 0.15mm cuvette (item b in the figure),

either no shift at all is evident, or a significantly smaller shift can be seen. Results of absorption measurements with the latter are given in the lower panel of Figure 2. As can be seen, the higher the BO21 concentration, the more significant the blue shift is – a finding which supports BO21 aggregation (which generates dimers, trimers and more complex formations of BO21) as the main cause of metachromasia.

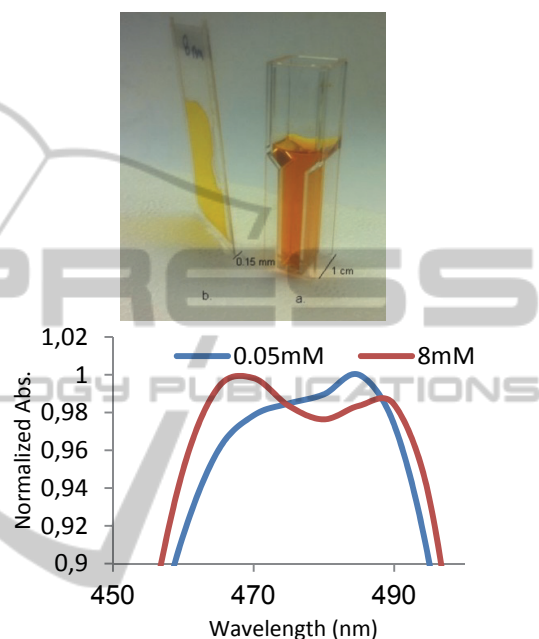


Figure 2: BO21 absorbance at high concentration. Upper panel: 8mM dye concentration in 10mm (a) and in 0.15mm (b) cuvettes. Lower panel: absorption spectra of 0.05mM BO21 (blue curve) and 8mM (red curve), as measured in the 0.15mm cuvette.

The level of blue shift was also found to be heparin concentration dependent, i.e. the higher the heparin concentration the greater the blue shift is (see Figure 3).

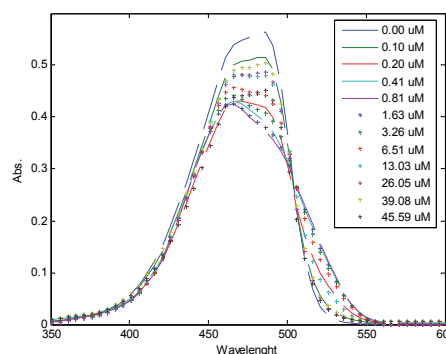


Figure 3: Absorption spectra of 10uM BO21 at various concentrations of heparin.

However, a close look into Figure 3 shows that the shift has a maximum at 0.8 μ M heparin, after which it decreases.

Our interpretation of these results follows Bradley's and Wolf's (1959). The idea is illustrated in Figure 4. Denoting BO21 as D and heparin binding site as P, we propose that at low heparin concentrations, namely $P/D < 1$, the heparin binding sites are completely occupied with BO21 and the surplus BO21 remains unbound in the solution (Figure 4a). In the case where $P/D \sim 1$ (Figure 4b), all BO21 molecules are expected to occupy all heparin binding sites and consequently, to yield maximum metachromasia. With further increase of the heparin concentration, $P/D > 1$ (Figure 4c), the competition between heparin molecules on BO21 molecules will finally lead to an equilibrium state where the BO21 molecules only partially occupy heparin binding sites, hence lessening the proximity between BO21 molecules attached to each of the heparin molecules and consequently lowering the chance for BO21 aggregation to occur on a single heparin.

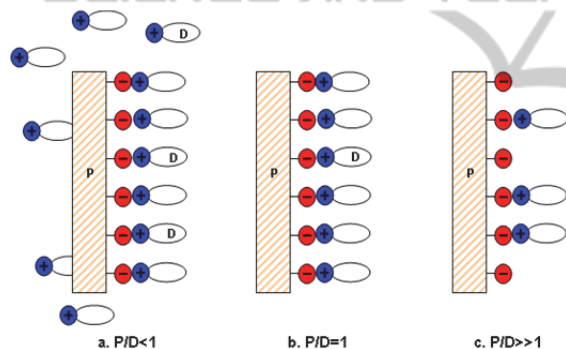


Figure 4: Aggregation schematic of the dye (D) on the anionic binding site of the polymer (P). a) Low polymer concentration leaves free dye molecules in the hosting solution. b) At an equal number of polymer binding sites and dyes, the dye molecules occupy all polymer binding sites. c) The number of polymer anionic binding sites is larger than that of dye molecules, hence yielding partial occupancy of the binding sites by the dye.

The experimental results and proposed mechanism was further strengthened by the use of computational chemistry. BO21 molecules is a multi-bodied electronic structure containing 47 nuclei and 169 electrons (despite the chlorine that dissolves in water), and therefore, the Schrödinger equation is impractical as a modelling method, hence, the Density Functional Theory (DFT) approach was applied (Hohenberg and Kohn 1964). DFT is a quantum mechanical modelling method which investigates the electronic structure (principally the ground state) of many-body systems.

With this theory, instead of using N wave function that depend on $3N$ coordination for x, y, z , the properties of a many-electron system can be determined by using the charge density ρ . This method is based on two Hohenberg-Kohn theorems (H-K). The first H-K theorem demonstrates that the ground state properties of a many-electron system are uniquely determined by an electron density that depends on only 3 spatial coordinates, while the second H-K theorem defines energy functional for the system, and proves that the correct ground state electron density minimizes this energy functional.

We calculated the electric dipole of the BO21 molecule. This molecule is cation due to a positive charge surrounding the nitrogen atom connected to the methyl group. Based on density function, a 3-d MEP (Molecular Electrostatic Potential) was produced in Figure 5a.

The molecule electric dipole moment μ was estimated by the formula:

$$\mu = - \int \rho(\mathbf{r}) \mathbf{r} d\tau + \sum_{\alpha=1}^{N_{nuc1}} Z_{\alpha} \mathbf{r}_{\alpha} \quad (2)$$

Where $\rho(\mathbf{r})$ is the density function, Z is atomic number and α is the nuclei index. The integral is above the electron coordinates and the summation yields the nucleus contribution to the dipole moment. The dipole moment vector of BO21 was found to be $\mu_{BO21} = 1.43 \times 10^{-29} \text{ C m}$, which is twice the water molecule ($\mu_{H_2O} = 6.2 \times 10^{-30} \text{ C m}$). $\vec{\mu}_{BO21}$ is indicated in Figure 5a by a light blue arrow in respect to the molecule axis. In order to support the aggregation theorem that causes the blue shift, we test the feasibility of dimer or trimer formation of BO21 molecules. In the tested model, the molecular electrical dipoles of dimers and trimers of BO21 are oriented in a parallel fashion as shown in Figure 5b. Surprisingly, the related binding energies were found to be even lower than those calculated for anti-parallel arrangements, a fact which explains the blue shift in the absorption spectrum.

2 OUTLINE OF OBJECTIVES

- To study the spectroscopic characteristics of BO21 in bulk solution in the presence and in the absence of biomolecules in general, as well as those which exist in leukocytes, in particular.
- To explore unique spectroscopic features of BO21 stained leukocytes, if they exist

- To correlate via the MCR, on same cell basis, between the explored spectroscopic features of BO21 stained sub types of leukocytes, and between traditional methods for differential leukocyte counts.

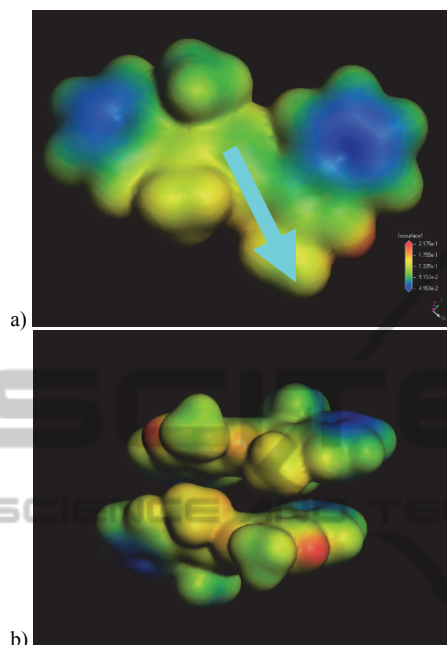


Figure 5: Molecular Electrostatic Potential from most negative (blue) to positive (red). a) BO21 monomer, electric dipole moment direction marked in light blue arrow. b) Parallel (dipoles) BO21 dimer.

3 RESEARCH PROBLEM

- Overcoming inner filter problem by the construction of unique cuvettes which will allow high concentration fluorescence and absorption measurements
- Development of theoretical tools for the examination of correctness level of the above unique cuvette performance
- Preparation of upright epifluorescence microscope for spectroscopic measurement of BO21-stained cells in a single cell resolution, while preserved within the MCR.
- Development of DFT-based algorithm for the investigation of dye-dye and dye-heparin interactions (primary results discussed above).
- Development of protocols for treatment of leukocytes within the MCR, e.g. cell loading, cell staining with BO21, fixation, Giemsa/Wright staining, etc.

- Evaluation of the diagnostic potential of BO21.

4 STATE OF THE ART

Presently, the leukocyte differential count test is mainly based on measuring individual cell electrical impedance, fluorescence and light scattering, which are all methods based on signals from an entire cell and not from the detailed image of a cell. Signals are acquired using flow cytometer and hematology analyzers that require large amounts of reagent and blood samples. Cell analysis on flow cytometers typically involves two steps: first, labeling target cells with detection assays, e.g. fluorophore-conjugated antibodies, and second, detecting target cells by corresponding optical signals, e.g., fluorescence assays (Yun et al., 2010) of fluorophore-conjugated antibodies for leukocyte analysis on the microflow cytometers. However, the low temperature needed for reagent storage makes this assay less than ideal for point-of-care applications. In comparison, assays of fluorescent dyes, have been proven as useful alternatives in cell analysis (Shi et al., 2013). Shi used the combination of FITC, PI and BO21 for classifying four types of leukocytes, though the spectroscopic aspect of BO21 was barely studied in respect to both FITC and PI. Furthermore, to the best of our knowledge, studies of BO21 fluorescence and its polarization do not exist.

5 RESEARCH METHODOLOGY

5.1 Bulk Spectroscopy of BO21

In this chapter we intend to further investigate spectroscopic features (Absorbance, FI and FP, fluorescence lifetime-FLT and polarization decay-PD) of BO21 in general, and at high concentrations in particular, in the absence and in the presence of heparin, in a variety of concentrations. This will be realized via our Cary UV spectrophotometer and Cary eclipse spectrofluorometer (Agilent, USA). In addition, FLT and PD and the evaluation of the rotational relaxation time of BO21 in solution will be realized via the DCS-120 confocal FLIM system (Becker and Hickl GmbH Berlin, Germany). Especially with the last type of measurements, which are time dependent, the extremely low quantum yield of fluorescence of BO21 (about 1000 times less than that of fluorescein), should be

carefully considered in order to improve the expected low S/N ratio.

Further investigation of the complexes: BO21 dimers (trimers) and BO21-heparin will be realized via Density Functional Theory (DFT). Initial computational quantum chemistry based calculations teach that the molecular electrical dipoles of BO21 in dimers and trimers tends to be parallel oriented. Moreover, and quite surprisingly, the related binding energies are even lower than those calculated for anti-parallel arrangements. The BO21-heparin complexes formed, seem to be governed by electrostatic interactions, wherein the positive charge of BO21 interacts with the negative charge located in the heparin sites. Additionally, the π -cation interaction between stacked BO21 molecules stabilizes the complexes. Quantum calculations were performed with the DMol3 module in Material Studio (Accelrys, USA).

5.2 Bulk Spectroscopy of BO21-stained Leukocytes Suspension

In this chapter we intend to repeat the bulk measurement discussed above, but in suspension of BO21 stained leukocyte, utilizing the Cary UV spectrophotometer and the Cary eclipse spectrofluorometer (Agilent, USA).

5.3 Single Cell Resolution Spectroscopy of BO21-stained Leukocytes

In this chapter we intend to measure the spectroscopic characteristics of intra leukocyte BO21 at a single-cell resolution. This will be carried out by loading the leukocytes in a Microtiter plate Cell Retainer (MCR). MCR is a high throughput Microtiter plate that has been developed in our Center (Deutsch et al., 2006) to enable high-content, time-dependent analysis of the same single non-adherent and non-anchored cells in a large cell population while bio-manipulating the cells. The identity of each cell in the investigated population is secured, even during bio-manipulation, by cell retention in a specially designed concave microlens (Figure 6), acting as a picoliter well. The MCR technique combines micro-optical features and microtiter plate methodology.

While solutions for fluorescence measurement at a single cell resolution is quite common, solutions for single cell absorption (1nm spectral resolution) is slow to appear. Hence, for the realization of the latter in a single cell resolution, we intend to extensively upgrade our Olympus upright BX61

microscope (Tokyo, Japan) to enable medium throughput absorption measurements of BO21 stained cell.

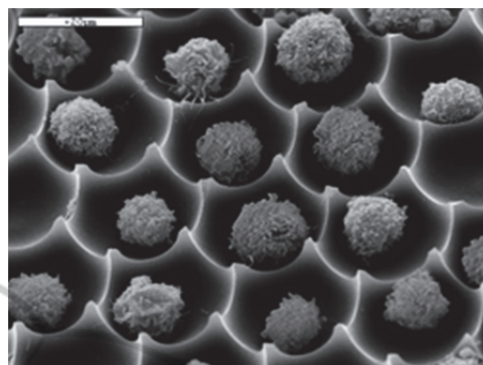


Figure 6: An SEM image of Jurkat T cells in MCR. Scale bar: 20.

In short, to the existing Olympus upright BX61 microscope, which is equipped with a sub-micron Marzhauser–Wetzlar motorized stage (types SCAN, with an Lstep controller, Wetzlar–Steindorf, Germany), a xenon lamp, 1nm spectral resolution monochromator, and a CCD camera will be added, adjusted and calibrated. The entire system will be controlled by designated / software. The captured images will be processed using Matlab (MathWorks, USA) to produce spectral quantile (SQ) maps, which present a surface plot showing absorption quantile amplitudes as a function of wavelength (see Figure 7).

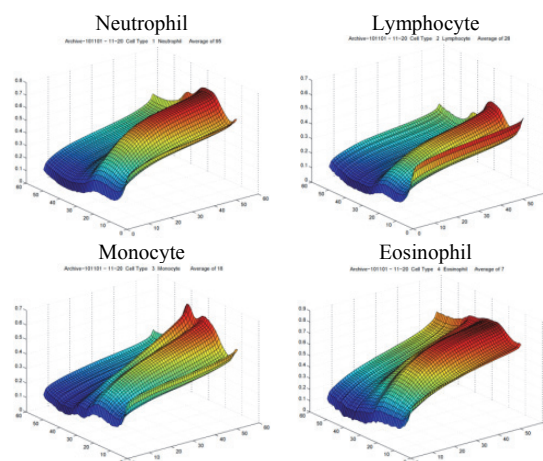


Figure 7: Spectral-Quantile (SQ) plots for four of the five normal leukocyte subtypes showing how BO21 metachromasia allows easy identification of the subtypes. Axis from left to right is the Quantile axis (50 quantiles). Axis from right to left is the wavelength axis (51 wavelengths from 400nm through 650nm at 5nm increments).

Finally, in order to explore possible identifying features which might be used for differentiating between types of leukocytes and between leukocytes and other type of cells, pre- versus post-fixation (with Wright Giemsa staining) correlation of BO21 stained cells will be performed.

6 EXPECTED OUTCOME

- Evaluating the ability of a single dye BO21 to classify types of leukocytes via maps of absorption, FI and FP spectra.
- Exploring the mechanism of BO21-Heparin interactions/structures in general, and that which stands behind the measured high FP of BO21 in water in particular.

REFERENCES

- Deutsch, M., Deutsch, A., Shirihai, O., Hurevich, I., Afrimzon, E., Shafran, Y., and Zurgil, N. (2006) 'A Novel Miniature Cell Retainer for Correlative High-Content Analysis of Individual Untethered Non-Adherent Cells'. *Lab on a Chip* 6 (8), 995–1000
- Hohenberg, P. and Kohn, W. (1964) 'Inhomogeneous Electron Gas'. *Physical Review* 136 (3B), B864–B871
- Kass, L. (1986) *Individual Leukocyte Determination by Means of Differential Metachromatic ...* 4581223. available from <<http://www.google.co.il/patents?id=RHk8AAAAEBAJ>> [3 February 2013]
- Shi, W., Guo, L., Kasdan, H., and Tai, Y.-C. (2013) 'Four-Part Leukocyte Differential Count Based on Sheathless Microflow Cytometer and Fluorescent Dye Assay'. *Lab on a Chip* [online] available from <<http://pubs.rsc.org/en/content/articlelanding/2013/lc/c3lc41059e>> [25 February 2013]
- Yun, H., Bang, H., Min, J., Chung, C., Chang, J. K., and Han, D.-C. (2010) 'Simultaneous Counting of Two Subsets of Leukocytes Using Fluorescent Silica Nanoparticles in a Sheathless Microchip Flow Cytometer'. *Lab on a Chip* 10 (23), 3243.